ACCSCIENCE PUBLISHING

Innovative Medicines & Omics

ORIGINAL RESEARCH ARTICLE

High inhibitory activity of flavonoids from *Sophora japonica* L. flower buds against α-amylase and α-glucosidase: A mechanistic insight

Jinting Sun[1†], Ranying Zhang[1†], Jiayan Xiong[1†], Jinlin Li[1], Chaoyang Zhang[1], and Yunfeng Ma[1,2,3*]

[1]Department of Bioengineering, School of Life Sciences, Henan University/Henan Province, China

[2]Institute of Microbial Engineering, Laboratory of Bioresource and Applied Microbiology, Henan University/Henan Province, China

[3]Engineering Research Center for Applied Microbiology of Henan Province/Henan Province, China

Abstract

In this work, a method was developed to screen compounds with enzyme activity inhibition *in vitro* using chromatographic analysis combined with activity difference analysis (CAADA). The flower buds of *Sophora japonica* L. (FBSJ) were found to contain abundant flavonoids. These flavonoids were then screened for their high inhibitory activity against α-amylase and α-glucosidase using fingerprint and activity difference analysis. Consistent conclusions were drawn from multiple techniques, including the reported technique, IC_{50} data, and CAADA. The inhibitory mechanism was further analyzed through enzyme inhibition kinetics, circular dichroism, fluorescence spectrometry, molecular docking, and molecular dynamics (MD). Among the six flavonoid components studied, quercetin was found to act as a competitive inhibitor against α-amylase, while kaempferol showed a mixed manner of inhibition against α-glucosidase. Molecular docking and MD simulations demonstrated that quercetin and kaempferol have higher binding energies and bound more tightly to their targets. In general, flavonols exhibited higher inhibitory activity than their corresponding flavonol glycosides against both α-amylase and α-glucosidase. Quercetin and kaempferol in FBSJ showed potential as inhibitors of α-amylase and α-glucosidase. This study not only presented a novel method for screening compounds with high activity but also provided a theoretical basis for studying the application and mechanism of flavonoids against α-amylase and α-glucosidase in FBSJ.

Keywords: *Sophora japonica* L.; Flavonoids; α-amylase; α-glucosidase

†*These authors contributed equally to this work.*

***Corresponding author:**
Yunfeng Ma
(mayunfeng@henu.edu.cn)

Citation: Sun J, Zhang R, Xiong J, Li J, Zhang C, Ma Y. High inhibitory activity of flavonoids *from Sophora japonica* L. flower buds against α-amylase and α-glucosidase: A mechanistic insight. *Innov Med Omics*. 2025;2(1):55-70. doi: 10.36922/imo.6010

Received: November 15, 2024
Revised: December 5, 2024
Accepted: December 13, 2024
Published online: December 30, 2024

Copyright: © 2024 Author(s). This is an Open Access article distributed under the terms of the Creative Commons Attribution License, permitting distribution, and reproduction in any medium, provided the original work is properly cited.

Publisher's Note: AccScience Publishing remains neutral with regard to jurisdictional claims in published maps and institutional affiliations.

1. Introduction

Flavonoids, polyphenolic compounds typically present in plants, play a crucial role in human nutrition, and numerous studies have thoroughly documented their various biological functions.[1] These compounds demonstrate multifunctional anti-diabetic properties by influencing certain cellular signaling pathways, thereby enhancing multiple facets of carbohydrate metabolism, including α-glycosidase activity, glucose

transport, aldose reductase activity, and cellular glucose uptake.[2-4] A practical strategy for controlling postprandial hyperglycemia involves using α-glucosidase and α-amylase inhibitors.[5] Implementing dietary strategies that incorporate flavonoids can help establish effective dietary recommendations for healthy individuals and aid in relieving symptoms for patients suffering from Type 2 Diabetes Mellitus.[6]

The flower buds of *Sophora japonica* L. (FBSJ), a form of traditional Chinese medicine (TCM), are common known as Flos Sophorae Immaturus, which are utilized for treating various ailments, including hypertension and arteriosclerosis. Flavonoids, such as quercetin, kaempferol, genistein, rutin, and isorhamnetin, have been isolated from *S. japonica* L.[7,8] The components found in TCM are intricate, with numerous chemicals contributing to its therapeutic efficacy. This intricacy poses challenges in identifying the specific active constituents of TCM. Nevertheless, high-performance liquid chromatography (HPLC)-based fingerprint spectra have been employed to thoroughly analyze the diversity and concentrations of compounds in botanical materials, thereby assessing the quality of TCM products.[9,10] Circular dichroism (CD), when paired with fluorescence quenching methods, is frequently used to examine how flavonoids interact with proteins, offering a crucial understanding of protein-ligand interactions, as well as the conformational and structural changes of flavonoids in relation to proteins.[11] Furthermore, molecular simulation methods, including molecular docking and dynamics, have become increasingly significant in studying interactions and have contributed to exploring the mechanisms behind inhibitor-enzyme interactions, enhancing our comprehension from a molecular biology standpoint regarding the efficacy of these interactions.[12]

Various screening methods have been developed and applied in a wide range of fields. However, these methods often require specialized software and complex data processing. Therefore, there is an urgent need to develop a simple and feasible screening and comparison method. Chromatographic analysis combined with activity difference analysis (CAADA) was applied. This article aimed to assess the inhibitory potentials of the extract against α-amylase and α-glucosidase and to develop a new screening method using compounds found in FBSJ. The compounds that exhibited significant inhibitory effects were verified, and the inhibitory mechanism was preliminarily studied.

2. Materials and methods

2.1. Materials

FBSJ was collected from the campus of Henan University. Porcine pancreas α-amylase and yeast α-glucosidase were purchased from Bomei Biochemical Co. (Hefei, Anhui Province, China). 4-Nitrophenyl-α-D-glucopyranoside (pNPG) was purchased from Beijing Kuerhuaxue Co (Beijing, China). Rutin, quercetin, kaempferol, isorhamnetin, kaempferol-3-O-rutinoside, and narcissoside were purchased from Chengdu Alfa Biotechnology Co (Chengdu, China). Acarbose tablets were purchased from Bayer Healthcare Co (Leverkusen, Germany).

2.2. Determination of flavonoids in samples

The active components of *S. japonica* L. were extracted using ethanol (5 g FBSJ: 100 mL solvent) at various concentrations of 30%, 50%, 70%, and 90%, as well as with ethyl acetate. Flavonoid standards were dissolved in methanol, while the flavonoid content in the samples was extracted using ethanol. These flavonoids were subsequently separated with a Waters HPLC system (Milford, Massachusetts, USA) equipped with a C18 Agilent column. The gradient elution was performed under the following conditions: (A) and 0.05% phosphoric acid (B), with the following time intervals: 0 – 10 min at 24 – 40% (A); 10 – 20 min at 40 – 50% (A); 20 – 35 min at 50 – 75% (A); 35 – 40 min at 75 – 80% (A); 40 – 50 min at 80 – 95% (A); 50 – 55 min at 95 – 95% (A); and 55 – 80 min at 95 – 24% (A). Both qualitative and quantitative analyses of the samples were conducted using standard solutions. The data were imported into the "Traditional Chinese Medicine Fingerprint Similarity Evaluation System," and then HPLC fingerprint spectra were obtained.

2.3. Inhibition activity assays of enzyme

2.3.1. The assessment of α-amylase inhibition activity

The assessment of α-amylase inhibition activity was conducted as described in previous studies, with necessary adjustments made.[13] Initially, 20 of samples at various concentrations were combined with 150 μL of α-amylase solution (0.58 U/mL) and incubated at 37°C for 5 min. Subsequently, 150 μL of 1% starch was added to the mixture, which was then incubated at 37°C for an additional 15 min. Finally, 250 μL of DNS reagent (dinitrosalicylic acid reagent, a reagent used for the determination of reducing sugar content, prepared by dissolving 18.2 g of potassium sodium tartrate in 50 mL of distilled water, heating, and sequentially adding 0.63 g of 3,5-dinitrosalicylic acid, 2.1 g of NaOH, and 0.5 g of phenol to the hot solution, stirring until dissolved, cooling, and diluting with distilled water to 100 mL, stored in a brown bottle at room temperature) was mixed, and the mixture was boiled for 5 min. After diluting the solution to an appropriate concentration, its absorbance was recorded at 540 nm using a microplate reader.

2.3.2. The assessment of α-glucosidase inhibition activity

The assessment of α-glucosidase inhibition activity was conducted as described in previous studies, with necessary adjustments made.[14] Initially, a mixture was prepared by adding 50 μL of α-glucosidase at a concentration of 2 U/mL, followed by 50 μL of the inhibitor at varying concentrations, and 80 μL of buffer solution. This mixture was incubated for 10 min at 37°C. Subsequently, 50 μL of pNPG (20 mM) was added, and the contents were mixed thoroughly and shaken. The reaction was allowed to continue at 37°C for 20 min, after which it was concluded by adding 100 μL of Na_2CO_3. The solution was then diluted to a suitable concentration, and the absorbance at 540 nm was measured with a microplate reader. The inhibition rate was calculated using the following equation:

$$\text{Inhibition rate}\% = 1 - [\frac{(A_3 - A_4)}{(A_1 - A_2)}] \times 100 \quad \text{(I)}$$

A^1 served as the blank group, consisting of enzyme and buffer, while A_2 acted as the blank control group, containing only the buffer. A_3 represented the sample group that included the enzyme and the inhibitor, and A_4 functions as the sample control group, which was made up of buffer and the inhibitor. The IC_{50} value indicated the concentration of the inhibitor needed to reduce the enzyme activity by half. Acarbose was established as a control substance.

2.4. Correlation analysis

The research focused on the concentration-effect relationships of various solvent extracts regarding their ability to inhibit the functions of α-amylase and α-glucosidase. Grey relation analysis (GRA) was performed using Statistical Package for the Social Sciences (SPSS) Pro, utilizing the peak areas obtained from the HPLC fingerprint profiles of the different extracts, in conjunction with the IC_{50} values associated with enzyme inhibition activities.[15,16] By examining the overlapping areas of the HPLC fingerprints and their corresponding IC_{50} values, CAADA was used to assess the peak areas of each constituent in relation to the IC_{50} values. This approach established a relationship between individual components and their enzyme inhibitory effects, while also proposing hypotheses about the compounds responsible for these inhibitory activities.

2.5. Kinetic assay for inhibition action

For the overall assessment of inhibition kinetics, the same procedures utilized for evaluating enzyme activity were applied. The Lineweaver–Burk plot was employed to analyze the inhibition type.[8] This plot was derived using specific equations:

$$\text{Competitive inhibition: } \frac{1}{v} = \frac{K_m}{V_{max}}\left(1 + \frac{[I]}{K_i}\right)\frac{1}{[S]} + \frac{1}{V_{max}} \quad \text{(II)}$$

$$\text{Uncompetitive inhibition: } \frac{1}{v} = \frac{K_m}{V_{max}}\frac{1}{[S]} + \frac{1}{V_{max}}\left(1 + \frac{[I]}{K_i}\right) \quad \text{(III)}$$

Noncompetitive inhibition:

$$\frac{1}{v} = \frac{K_m}{V_{max}}\left(1 + \frac{[I]}{K_i}\right)\frac{1}{[S]} + \frac{1}{V_{max}}\left(1 + \frac{[I]}{K_i}\right) \quad \text{(IV)}$$

$$\text{Mixed inhibition: } \frac{1}{v} = \frac{K_m}{V_{max}}\left(1 + \frac{[I]}{K_i}\right)\frac{1}{[S]} + \frac{1}{V_{max}}\left(1 + \frac{[I]}{K_{is}}\right) \quad \text{(V)}$$

$$\text{Slope} = \frac{K_m}{V_{max}}\left(1 + \frac{[I]}{K_i}\right) \quad \text{(VI)}$$

$$Y_{intercept} = \frac{1}{V_{max}}\left(1 + \frac{[I]}{K_{is}}\right) \quad \text{(VII)}$$

Where v is the reaction rate; K_m, K_i, and K_{is} represent the Michaelis-Menten, free and bound enzyme inhibition constants, respectively; [S] stands for substrate concentration; [I] represents the concentration of the inhibitor.

2.6. Characterization method

2.6.1. Fluorescence spectrum analysis

A fluorescence quenching test was conducted to study the interaction between flavonoids in FBSJ and α-amylase or α-glucosidase, with slightly modifications.[17] α-amylase (0.58 U/mL) and α-glucosidase (2 U/mL) were incubated with different concentrations of quercetin/kaempferol in the water bath at 298 K, 304 K, and 310 K for 5 min. Measurements were performed under an excitation wavelength of 280 nm and a scanning wavelength range of 300 – 500 nm, with both the excitation and emission slit widths set to 5.0 nm. The information about K_{SV}, K_q, and K_a and quenching type derived from the Stern-Volmer equation as follows:

$$F_0 / F = 1 + K_{sv}[Q] = 1 + K_q\tau_0[Q] \quad \text{(VIII)}$$

$$\lg\frac{F_0 - F}{F} = \lg K_a + n\lg[Q] \quad \text{(IX)}$$

Where F_0 and F represent the fluorescence intensities with or without flavonoids, respectively, and τ_0 is 10^{-8} s; K_{SV}, and K_q represent the quenching constants and diffusion collision quenching rate constants, respectively; [Q] represents the concentration of flavonoids.

2.6.2. Calculation of thermodynamic parameters

The temperature-dependent interactions were investigated by calculating the interactions between inhibitors and enzymes using the following equations:

$$\ln K_a = -\frac{1}{T}\left(\frac{\Delta H}{R}\right) + \frac{\Delta S}{R} \quad (X)$$

$$\Delta G° = \Delta H° - T\Delta S° = -RT\ln K_a \quad (XI)$$

Where K_a ($Lmol^{-1}$) is the binding constant, R (8.314 J mol^{-1} K^{-1}) is the gas constant, $\Delta S°$ and $\Delta H°$ represent the values used to evaluate the binding force, and $\Delta G°$ indicates the spontaneity of the interaction.

2.6.3. CD spectrum analysis

The α-amylase and α-glucosidase were mixed with flavonoid samples in different proportions and scanned by CD spectroscopy. The combined solutions were scanned across a wavelength range of 190 – 260 nm. The results of the measurements were then calculated using CDNN software (Aviv Biomedical Inc., Lakewood, USA).

2.7. Molecular docking

Molecular docking simulations were carried out using AutoDock 4.0. The structures of flavonoid compounds were downloaded from PubChem. The protein data for α-amylase (PDB ID: 1OSE) were obtained from the Protein Data Bank, and α-glucosidase was obtained from homology modeling. Before docking, the enzyme structures were prepared by removing all water molecules, adding hydrogen atoms, and distributing the Gasteiger charges to generate the PDBQT file. Finally, the docked complexes were visualized and analyzed by PyMOL.[18,19]

2.8. Molecular dynamics (MD)

MD simulations at 100 ns were performed using GROMACS 2020. The Amber99 SB force field was applied to the proteins in this study, and the topologies of a-amylase and α-glucosidase were prepared using the pdb2gmx module of GROMACS 2020. The topology and coordinate parameter files for quercetin and kaempferol were generated through simulation on the ACPYPE server (https://www.bio2byte.be/acpype/status/). The physiological environment of the proteins was simulated by adding the TIP3P aqueous model to the protein complex system, which was solvated using dodecahedral boxes, with sodium ions added to neutralize the overall charge. The simulations were performed using the conjugate gradient method combined with the most rapid descent method for 50,000 steps each to minimize energy. The V-rescale thermostat was used for temperature coupling to obtain a correct trajectory distribution of the canonical ensemble. The Berendsen pressure control method was used to slowly heat the system temperature to 300 K within 10 ns. After heating, the NPT ensemble (T = 300 K and P = 1 atm) was used for 100 ns simulation under periodic boundary conditions.[20]

2.9. Statistical analysis

All data were analyzed and presented as the mean ± standard deviation of the results. Three experiments were performed for each data set. All statistical analyses were carried out using SPSS 19.0 (IBM Corp. Armonk, NY, USA) and GraphPad Prism 8 (GraphPad, San Diego, USA) to evaluate the significance of differences.

3. Results

3.1. Identification of flavonoids in FBSJ and establishment of HPLC fingerprint

Figure 1 shows the fingerprints of flavonoids in FBSJ extracted with different solvents. A total of six common peaks were calibrated from the six samples. Compared with the peak diagram of the reference substance, the six components were identified as rutin, kaempferol-3-O-rutinoside, narcissoside (isorhamnetin-3-O-rutoside), quercetin, kaempferol, and isorhamnetin according to the peak times, which was consistent with previous reports.[21,22] The flavonoids in FBSJ include three flavonols and their corresponding flavonol glycosides, which contributed to comparing the activities of flavonols and their corresponding glycosides. Combined with the fingerprints, it was evident that the main chromatographic peak was rutin in various ethanol solutions extract of FBSJ, while the main chromatographic peak was quercetin in ethyl acetate extract of FBSJ. It was shown that the extraction of FBSJ with different solvents resulted in varying enzyme inhibition rates (expressed by the half inhibition rate concentration, IC_{50}). The order of α-amylase inhibition rates was ethyl acetate >30% ethanol >90% ethanol >50% ethanol >70% ethanol >water. The order of α-glucosidase inhibition rate was ethyl acetate >70% ethanol >90% ethanol >50% ethanol >30% ethanol >water (Table 1). The inhibition effect of the ethyl acetate extract of FBSJ was significant compared to the other extracts, although acarbose showed the most obvious inhibition. Based on the data in Figure 1, quercetin was the main constituent in ethyl acetate, which suggests that quercetin may be the favorite natural compound responsible for the inhibitory activity.

3.2. Correlation analysis

The peak areas of six common peaks, represented by P1-P6, were established as the comparison sequence, with the IC_{50} values for enzyme inhibition as the reference sequence.[23] According to references,[24-26] using the enzyme inhibition rate as a pharmacodynamic index, the results are shown in Table 2. The correlation order with α-amylase was P5, P4, P3,

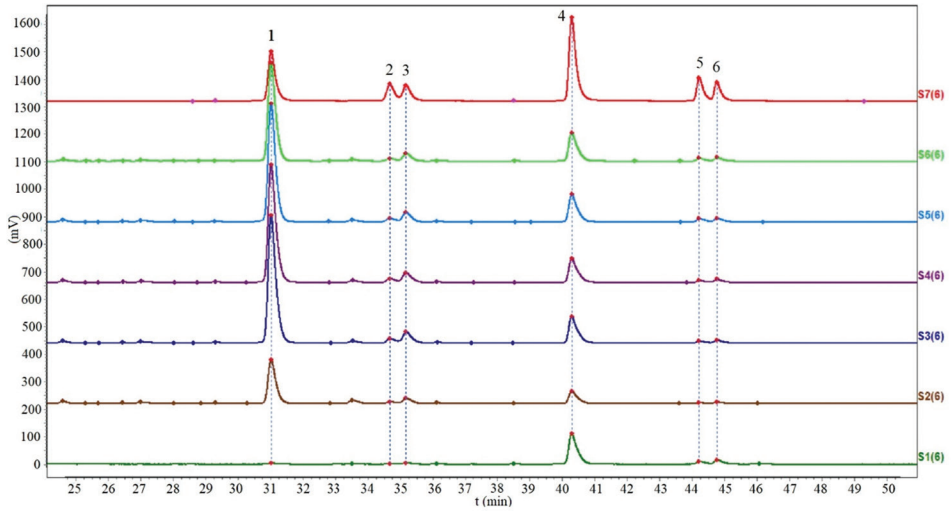

Figure 1. High-performance liquid chromatography fingerprint of extracts with different solvents. S1: Ethyl acetate extract, S2: Water extract, S3: 90% ethanol extract, S4: 70% ethanol extract, S5: 50% ethanol extract, S6: 30% ethanol extract, S7: Flavonoids standard mixed solution (Peak 1: Rutin, Peak 2: Kaempferol-3-rutinoside, Peak 3: Narcissoside, Peak 4: Quercetin, Peak 5: Kaempferol, Peak 6: Isorhamnetin).

Table 1. Inhibition effects of different extracts of FBSJ on enzymes

Samples	α-amylase inhibition IC_{50} (mg/mL)	α-glucosidase inhibition IC_{50} (mg/mL)
Acarbose	0.95±0.01	0.00033±0.0001
30% ethanol extract	13.59±0.03	0.63±0.02
50% ethanol extract	14.68±0.05	0.61±0.01
70% ethanol extract	20.09±0.12	0.29±0.02
90% ethanol extract	14.36±0.03	0.43±0.03
Ethyl acetate extract	10.16±0.01	0.09±0.01
Water extract	44.26±0.16	0.94±0.03

Abbreviation: FBSJ: Flower buds of *Sophora japonica* L.

P6, P2, and P1, while the correlation order with α-glucosidase was P5, P4, P6, P3, P2, and P1. Among the six characteristic peaks of the HPLC pattern, the correlations of peaks were all >0.6, indicating that the inhibition of both enzyme's activities by FBSJ was jointly exerted.[27] Peak P4 (quercetin), peak P5 (kaempferol), and peak P6 (isorhamnetin) were more closely related, indicating that quercetin, kaempferol and isorhamnetin might have a better inhibitory effect. The use of CAADA was an integrated method to assess the changes in the content of each substance in different solvent extracts and their corresponding enzyme inhibition activity. By comparing the changes in each substance across different solvent extracts and the total inhibition rate (up- or down-regulation), and according to the significant difference (*P*-value) of the peak areas of the fingerprint profiles of different solvent extracts, the results were evaluated. If the change of the substance and the change of the total inhibition rate were the same and $P < 0.01$ scored 2 points, and $P < 0.05$ scored 1 point, on the contrary, the opposite change scored −1 point. The results, shown in Tables 3-5, indicate that the highest scores were obtained for P4, P5, and P6, indicating that quercetin, kaempferol, and isorhamnetin had significant effects on the inhibition of both enzyme's activities. From the above results, the CAADA findings were in general agreement with the GRA and the IC_{50} values of each substance, indicating the reliability of CAADA and its relative simplicity and ease of operation.[28,29] Except for isorhamnetin, the result of the new method closely matched those of the GPA and IC_{50}, likely due to the lower concentration of isorhamnetin causing a system error. This analysis led to the conclusion that quercetin and kaempferol might be better inhibitors of both enzymes. From the IC_{50} values of each flavonoid, it was inferred that flavonols exhibited greater inhibitory activity than their corresponding flavonol glycosides against α-amylase and α-glucosidase under the same conditions, which is consistent with the structural requirements for enzyme activity reported in previous studies.[30]

3.3. Inhibition types of flavonoids

The inhibitory kinetics of kaempferol and quercetin against the enzymes α-amylase and α-glucosidase were investigated using Lineweaver–Burk plots to determine the type of inhibition.[31,32] As shown in Figure 2A-D, the Lineweaver–Burk plot for quercetin demonstrated several lines intersecting on the y-axis, showing that quercetin acts as a competitive inhibitor of α-amylase. Conversely, the plots for α-glucosidase revealed intersections in the second or third quadrants, indicating that quercetin inhibits α-glucosidase in a mixed inhibition manner.

Table 2. IC_{50} values and GRA analysis of flavonoids from FBSJ extracts

Peak	α-amylase		α-glucosidase	
	Correlation coefficient	IC_{50} (mg/mL)	Correlation coefficient	IC_{50} (mg/mL)
P5 (Kaempferol)	0.787	0.33±0.05	0.678	0.19±0.05
P4 (Quercetin)	0.783	0.29±0.03	0.669	0.06±0.01
P6 (Isorhamnetin)	0.777	1.1±0.10	0.664	0.21±0.06
P3 (Narcissoside)	0.781	>5	0.644	5.04±0.02
P2 (Kaempferol-3-rutinoside)	0.777	>5	0.64	3.00±0.03
P1 (Rutin)	0.772	ND	0.626	0.99±0.01

Abbreviations: ND: No activity detected; GRA: Grey relation analysis.

Table 3. Comparative index of different solvent extracts of various substances and inhibition of α- amylase activity

	30% ethanol	50% ethanol	70% ethanol	90% ethanol	Ethyl acetate	Water
30% ethanol	--	1↑2 ↑ 3↑4 ↓ 5↑6 ↑ I↓**	1↑2 ↑ 3↑4 ↓ 5↓6 ↓ I↓**	1↑2 ↑ 3↑4 ↓ 5↓6 ↓ I↓**	1↓2 ↓ 3↓4 ↑ 5↓6 ↑ I↑**	1↓2 ↓ 3↓4 ↓ 5↓6 ↓ I↓**
50% ethanol	--	--	1↑2 ↑ 3↑4 ↓ 5↓6 ↓ I↓**	1↑2 ↑ 3↑4 ↓ 5↓6 ↓ I↑**	1↓2 ↓ 3↓4 ↑ 5↓6 ↑ I↑**	1↓2 ↓ 3↓4 ↓ 5↓6 ↓ I↓**
70% ethanol	--	--	--	1↑2 ↑ 3↑4 ↑ 5↓6 ↓ I↑**	1↓2 ↓ 3↓4 ↑ 5↑6 ↑ I↑**	1↓2 ↓ 3↓4 ↓ 5↓6 ↓ I↓**
90% ethanol	--	--	--	--	1↓2 ↓ 3↓4 ↑ 5↑6 ↑ I↑**	1↓2 ↓ 3↓4 ↓ 5↓6 ↓ I↓**
ethyl acetate	--	--	--	--	--	1↓2 ↓ 3↓4 ↓ 5↓6 ↓ I↓**
water	--	--	--	--	--	--

Note: 1=Rutin; 2=Kaempferol-3-O-rutinoside; 3=Narcissoside; 4=Quercetin; 5=Kaempferol; 6=Isorhamnetin; I=inhibition; ↑/↓ = contrast peak area or inhibition activity rise or fall. *P<0.05, **P<0.01.

Table 4. Comparative index of different solvent extracts of various substances and inhibition of α-glucosidase activity

	30% ethanol	50% ethanol	70% ethanol	90% ethanol	Ethyl acetate	Water
30% ethanol	--	1↑2 ↑ 3↑4 ↓ 5↑6 ↑ I↑*	1↑2 ↑ 3↑4 ↓ 5↓6 ↓ I↑**	1↑2 ↑ 3↑4 ↓ 5↓6 ↓ I↑**	1↓2 ↓ 3↓4 ↑ 5↓6 ↑ I↑**	1↓2 ↓ 3↓4 ↓ 5↓6 ↓ I↓**
50% ethanol	--	--	1↑2 ↑ 3↑4 ↓ 5↓6 ↓ I↓**	1↑2 ↑ 3↑4 ↓ 5↓6 ↓ I↑**	1↓2 ↓ 3↓4 ↑ 5↓6 ↑ I↑**	1↓2 ↓ 3↓4 ↓ 5↓6 ↓ I↓**
70% ethanol	--	--	--	1↑2 ↑ 3↑4 ↑ 5↓6 ↓ I↓**	1↓2 ↓ 3↓4 ↑ 5↑6 ↑ I↑**	1↓2 ↓ 3↓4 ↓ 5↓6 ↓ I↓**
90% ethanol	--	--	--	--	1↓2 ↓ 3↓4 ↑ 5↑6 ↑ I↑**	1↓2 ↓ 3↓4 ↓ 5↓6 ↓ I↓**
Ethyl acetate	--	--	--	--	--	1↓2 ↓ 3↓4 ↓ 5↓6 ↓ I↓**
Water	--	--	--	--	--	--

Note: 1=Rutin; 2=Kaempferol-3-O-rutinoside; 3=Narcissoside; 4=Quercetin; 5=Kaempferol; 6=Isorhamnetin; I=inhibition; ↑/↓ =contrast peak area or inhibition activity rise or fall. *P<0.05, **P<0.01.

Table 5. Integral method score table

Compound	α-amylase (score)	α-glucosidase (score)
P4 (Quercetin)	27	15
P5 (Kaempferol)	15	14
P6 (Isorhamnetin)	21	20
P4 (Rutin)	6	11
P2 (Kaempferol-3-O-rutinoside)	6	11
P3 (Narcissoside)	6	11

Similarly, kaempferol exhibited a mixed inhibition manner for both α-amylase and α-glucosidase.[33,34] The linear relationship between the slope and inhibitor concentration (as shown in the insets of Figure 2A-D) proving that these flavonoids bind to a single inhibition site on α-amylase and α-glucosidase.[35]

The K_i and K_{is} values for quercetin, kaempferol, and their interactions with the two enzymes were calculated according to equations (2) – (7).[36] The pertinent outcomes were displayed in Table 6. For kaempferol, the K_i value was lower than the K_{is} value, suggesting that kaempferol binds more tightly to α-amylase and α-glucosidase than the enzyme-substrate interaction. However, quercetin inhibited α-amylase competitively, indicating that quercetin binds directly to α-amylase and competes with the substrate. For

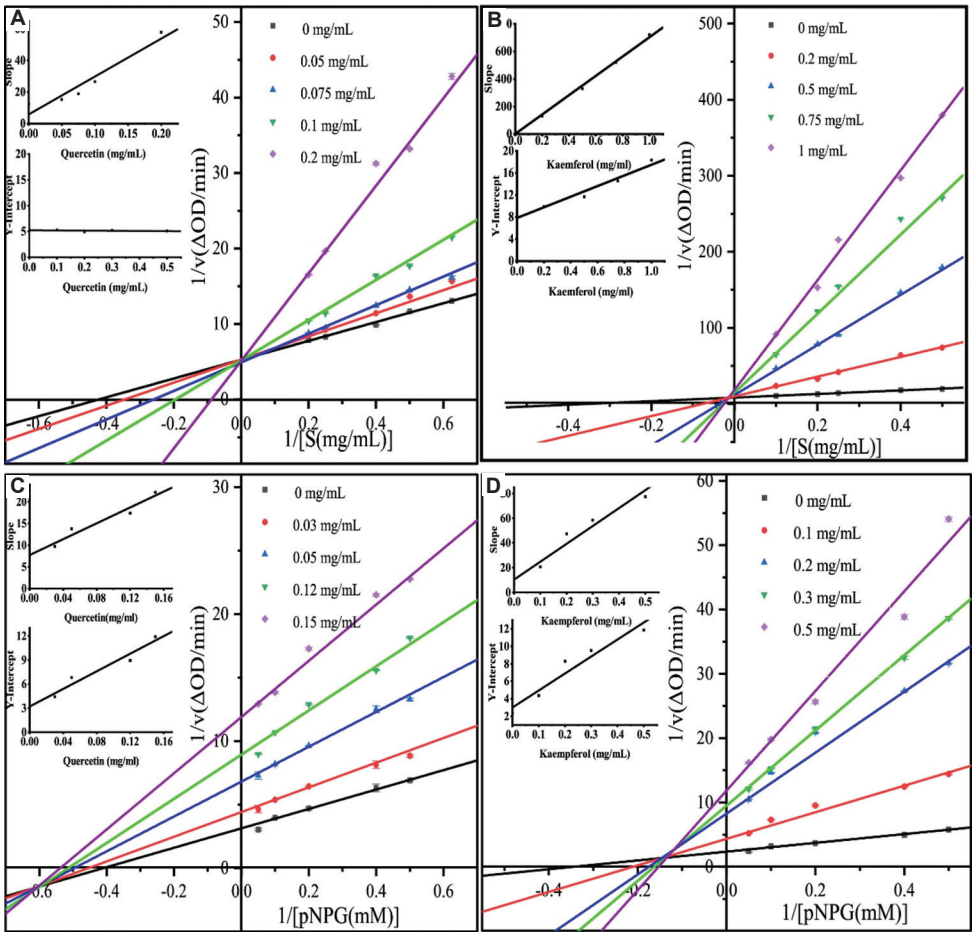

Figure 2. The inhibition kinetics of α-amylase by quercetin (A) and kaempferol (B), and α-glucosidase by quercetin (C) and kaempferol (D), as depicted by Lineweaver–Burk plots. The flavonoid concentrations used are indicated in the corresponding legend entries. The secondary plots (in the insets) show the linear relationship between the slope and y-intercept against the flavonoid concentration for each enzyme and inhibitor combination.
Abbreviation: pNPG: 4-Nitrophenyl-α-D-glucopyranoside.

quercetin, the K_i values (0.085 ± 0.002 mg/mL) were higher than the K_{is} values (0.058 ± 0.007 mg/mL), indicating that α-glucosidase binds stronger to the substrate complex than to the free enzyme.[37]

3.4. Fluorescence quenching

Figure 3 shows the fluorescence emission spectra of quercetin and kaempferol at different temperatures with α-amylase and α-glucosidase. The fluorescence intensity gradually reduced with increasing concentrations of quercetin and kaempferol, suggesting a noticeable impact of the inhibitors on both α-amylase and α-glucosidase.[38] The fluorescence intensity of the inhibitor's binding to the enzyme decreases with increasing inhibitor concentration, suggesting a more pronounced quenching effect on the enzymes.

Stern-Volmer analysis was performed to determine the quenching mechanism and binding constants. Quenching mainly occurs through two mechanisms between inhibitors and enzymes, including static and dynamic.[39] Using the equations (8) – (9), F_0/F pair [Q] plots were generated to calculate the values.[12,40] The K_q values were all $>2 \times 10^{10}$ L $mol^{-1}s^{-1}$, and these values gradually decreased with increasing temperature (Table 7). This suggested that the quenching mechanism of quercetin and kaempferol

Table 6. Detailed kinetic parameters of quercetin and kaempferol

Concentrations	K_i (mg/mL)	K_{is} (mg/mL)	Inhibition type
α-amylase			
Quercetin	0.024±0.003	-	Competitive
Kaempferol	0.036±0.0003	0.051±0.006	Mixed
α-glucosidase			
Quercetin	0.085±0.002	0.058±0.007	Mixed
Kaempferol	0.071±0.003	0.155±0.012	Mixed

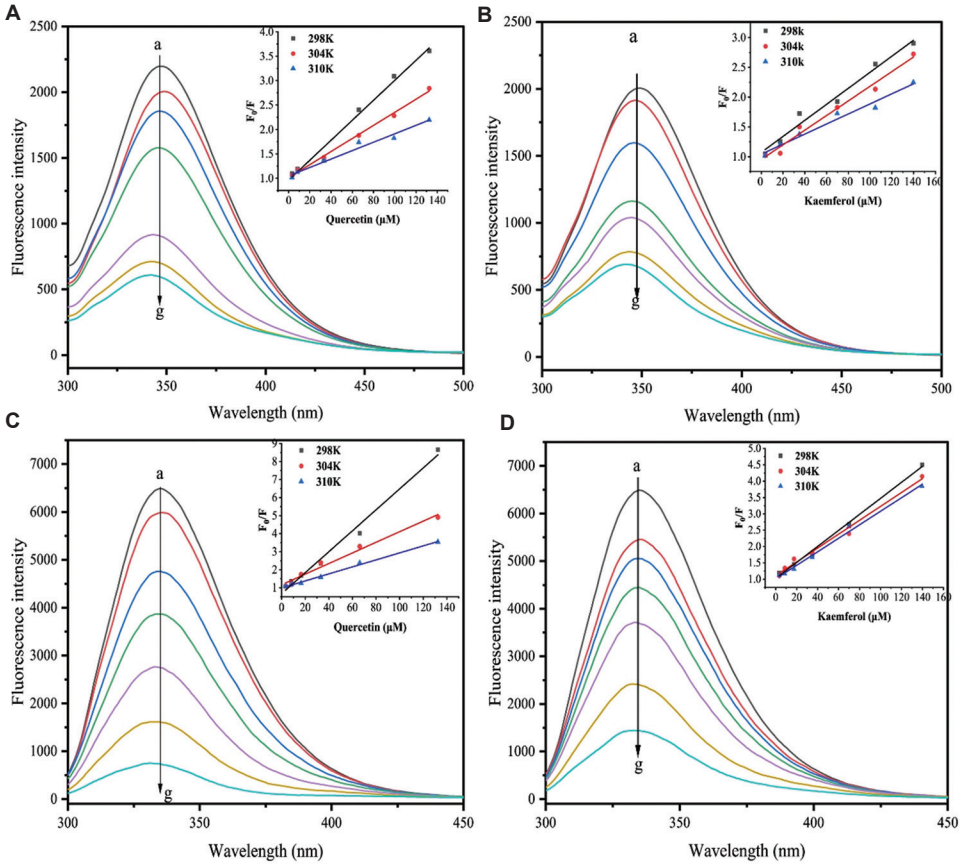

Figure 3. Fluorescence quenching of quercetin and kaempferol on α-amylase/α-glucosidase. (A) Fluorescence quenching spectra of α-amylase caused by quercetin at 298 K, with concentrations of 0, 3.31, 8.28, 16.56, 33.11, 66.22, 132.45 × 10^{-6} mol/L from (curves a to g). (B) Fluorescence quenching spectra of α-amylase caused by kaempferol at 298 K, with concentrations of 0, 3.49, 8.73, 17.47, 34.94, 69.87, 139.75 × 10^{-6} mol/L (curves a to g). (C) Fluorescence quenching spectra of α-glucosidase caused by quercetin at 298 K, with concentrations of 0, 3.31, 8.28, 33.11, 66.22, 99.34, 132.45 × 10^{-6} mol/L (curves a to g). (D) Fluorescence quenching spectra of α-glucosidase caused by kaempferol at 298 K, with concentrations of 0, 3.49, 17.47, 34.94, 69.87, 104.81, 139.75 × 10^{-6} mol/L (curves a to g). The secondary plot represents the Stern-Volmer plot (insets in each panel).

was static. The K_a values of quercetin and kaempferol considerably altered with rising temperature and were consistent with the change of K_{sv} values. This indicated that quercetin and kaempferol form complexes with enzymes, which decreased in stability as the temperature increased. This was probably due to the inhibition of endogenous fluorescence caused by the formation of these enzyme-inhibitor complexes. Both quercetin and kaempferol exhibited binding sites close to 1, suggesting a single type of binding site.[1] This observation was consistent with the kinetic results.

3.5. Thermodynamic parameters

Typically, small molecules interact with enzymes non-covalently, and these interactions can be calculated by thermodynamic parameters including electrostatic interactions, hydrogen bonding, van der Waals forces, and hydrophobic interactions. Negative ΔG^{o} values imply that the binding of quercetin and kaempferol to α-amylase and α-glucosidase was a spontaneous process. The calculated negative $\Delta H°$ value indicates the interaction between quercetin and kaempferol and both enzymes was an exothermic process (Table 7). In addition, $\Delta H° < 0$ and $\Delta S° < 0$ demonstrate that hydrogen binding and van der Waals forces are the principal forces driving the binding of quercetin and kaempferol to both enzymes. This aligns with the guidelines proposed by Ross and Subramanian.[41,42]

3.6. CD spectra analysis

CD is an effective tool for examining protein conformational changes induced by ligands. As shown in Figure 4, α-amylase and α-glucosidase exhibit two negative bands at approximately 207 and 228 nm, and 208 and 220 nm, respectively.[43] For α-amylase, the α-helix content increased from 14.25% to 14.72% (quercetin), 14.57% (kaempferol), 15.50% (isorhamnetin), 15.35% (rutin), 15.93% (kaempferol-3-O-rutinoside), and 15.90% (narcissoside), while the β-sheet content decreased from

Table 7. Binding constants, binding sites, thermodynamic parameters of quercetin and kaempferol with α-amylase and α-glucosidase at 298 K, 304 K, and 310 K

System	T (K)	K_q ($\times10^{12}$ $Lmol^{-1}$)	K_a ($\times10^{4}$ $Lmol^{-1}$)	*n*	ΔH^o (KJ mol^{-1})	ΔG^o (KJ mol^{-1})	ΔS^o (J $mol^{-1}k^{-1}$)
Quercetin-α-amylase	298 K	2.04±0.02	0.83±0.03	0.91	−60.39±2.52	−22.41±1.02	−127.45±3.52
	304 K	1.34±0.03	0.54±0.02	0.90		−21.65±2.54	
	310 K	0.86±0.02	0.32±0.01	0.88		−20.88±1.32	
Kaempferol-α-amylase	298 K	1.35±0.05	1.51±0.02	1.00	−126.08±4.57	−24.48±0.58	−340.96±5.76
	304 K	1.23±0.03	1.20±0.04	1.25		−22.43±1.24	
	310 K	0.85±0.03	0.21±0.01	1.20		−20.38±2.65	
Quercetin-α-glucosidase	298 K	5.81±0.02	25.12±0.22	1.17	−204.95±3.68	−30.71±3.02	−584.70±6.52
	304 K	2.94±0.01	4.37±0.04	1.02		−27.21±1.61	
	310 K	1.94±0.03	1.02±0.02	0.94		−23.69±4.32	
Kaempferol-α-glucosidase	298 K	2.45±0.04	0.33±0.03	0.80	−168.35±5.09	−19.75±2.32	−498.67±6.35
	304 K	2.12±0.04	0.05±0.04	0.85		−16.75±2.65	
	310 K	2.07±0.03	0.02±0.02	0.90		−13.76±1.53	

Table 8. The contents of secondary structures of α-amylase and α-glucosidase in *Sophora japonica* L

The ratio of enzymes to flavanoids	α-helix (%)	β-sheet (%)	β-turn (%)	Random coil (%)
α-amylase	14.25	47.46	11.92	26.45
α-amylase: Quercetin=4:1	14.72	46.16	12.13	26.92
α-amylase: Kaempferol=4:1	14.57	46.16	11.84	27.42
α-amylase: Isorhamnetin=4:1	15.50	45.92	12.88	25.76
α-amylase: Rutin=4:1	15.35	42.81	11.81	29.25
α-amylase: Kaempferol-3-O-rutinoside=4:1	15.93	42.49	12.44	29.21
α-amylase: Narcissoside=4:1	15.9	41.97	12.23	30.05
α-glucosidase	24.54	24.30	15.11	37.05
α-glucosidase: Quercetin=3:1	23.47	27.00	14.89	36.19
α-glucosidase: Kaempferol=3:1	22.66	28.90	14.67	35.84
α-glucosidase: Isorhamnetin=3:1	23.13	28.10	14.79	35.77
α-glucosidase: Rutin=3:1	22.51	28.30	14.23	36.93
α-glucosidase: Kaempferol-3-O-rutinoside=3:1	23.16	27.00	14.41	37.10
α-glucosidase: Narcissoside=3:1	22.77	27.20	14.25	37.49

the initial content of 47.46 – 46.16% (quercetin), 46.16% (kaempferol), 45.92% (isorhamnetin), 42.81% (rutin), 42.49% (kaempferol-3-O-rutinoside), and 45.92% (narcissoside) (Table 8). For α-glucosidase, the α-helix content decreased from 24.54% to 23.47% (quercetin), 22.66% (kaempferol), 23.13% (isorhamnetin), 22.51% (rutin), 23.16% (kaempferol-3-O-rutinoside), and 22.77% (narcissoside). However, the β-sheet content increased

from the initial content of 24.30% to 27.00% (quercetin), 28.90% (kaempferol), 28.10% (isorhamnetin), 28.30% (rutin), 27.00% (kaempferol-3-O-rutinoside), and 27.20% (narcissoside), possibly due to alterations in enzyme activity and structure caused by the inhibitors.[44] These results suggest that flavonoid compounds induced changes in the secondary structure of enzymes, blocking the formation of active sites or hindering substrate binding, thereby affecting the activity of enzymes.[45,46] This is consistent with the fluorescence data, which showed that these substances impacted the enzyme's structure and suggested that they affected the enzyme activity.

3.7. Molecular docking analysis

The 3D structure of α-glucosidase derived from homology modeling was assessed using Verify-3D assay, which revealed that 95.35% of the amino acid residues had an average 3D/one-dimensional fraction ≥0.2. This indicated that 95.35% of the target amino acid sequence was compatible with other amino acid residues (Figure 5). The detection results of Ramachandran plot program showed that 99.6% of the residues in the model were in the optimal and permissive regions, with 89.7% in the optimal region and 9.9% were in the permissive region. These findings indicate the reasonable distribution of amino acid dihedral angles in the model, confirming its reliability and accuracy.

To further understand the binding pattern of the flavonoid components of FBSJ, we used molecular docking to mimic the interaction of the compounds with α-amylase and α-glucosidase. The optimal binding active component was determined based on the binding energy generated during the docking process. A higher binding energy indicates a more stable complex with tighter binding. The molecular docking results showed that quercetin and kaempferol had the highest binding energies for both enzymes. The binding energies for quercetin and kaempferol

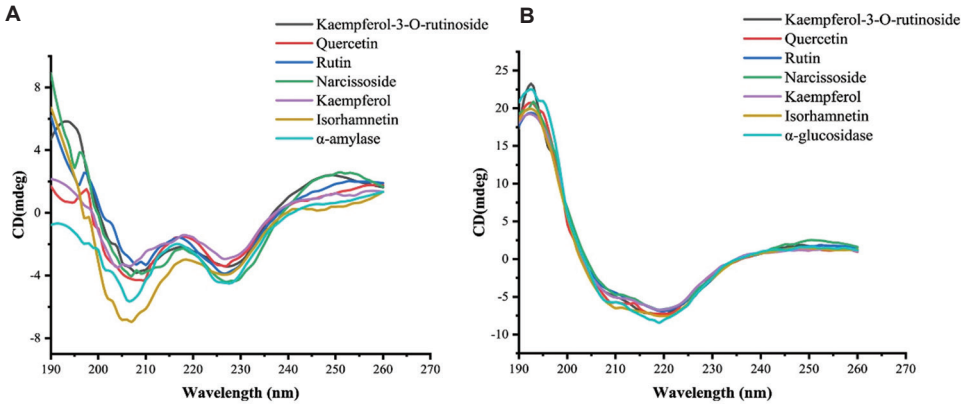

Figure 4. CD spectra of flavonoids-α-amylase/α-glucosidase systems. (A) Flavonoids-α-amylase; (B) Flavonoids-α-glucosidase. Abbreviations: CD: Circular dichroism; mdeg: Millidegree.

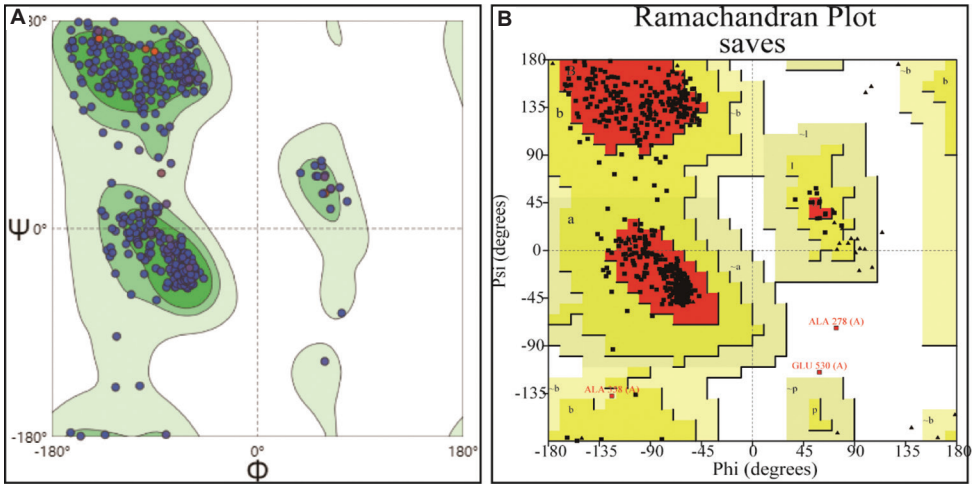

Figure 5. (A and B) Ramachandran plot model quality evaluation diagram

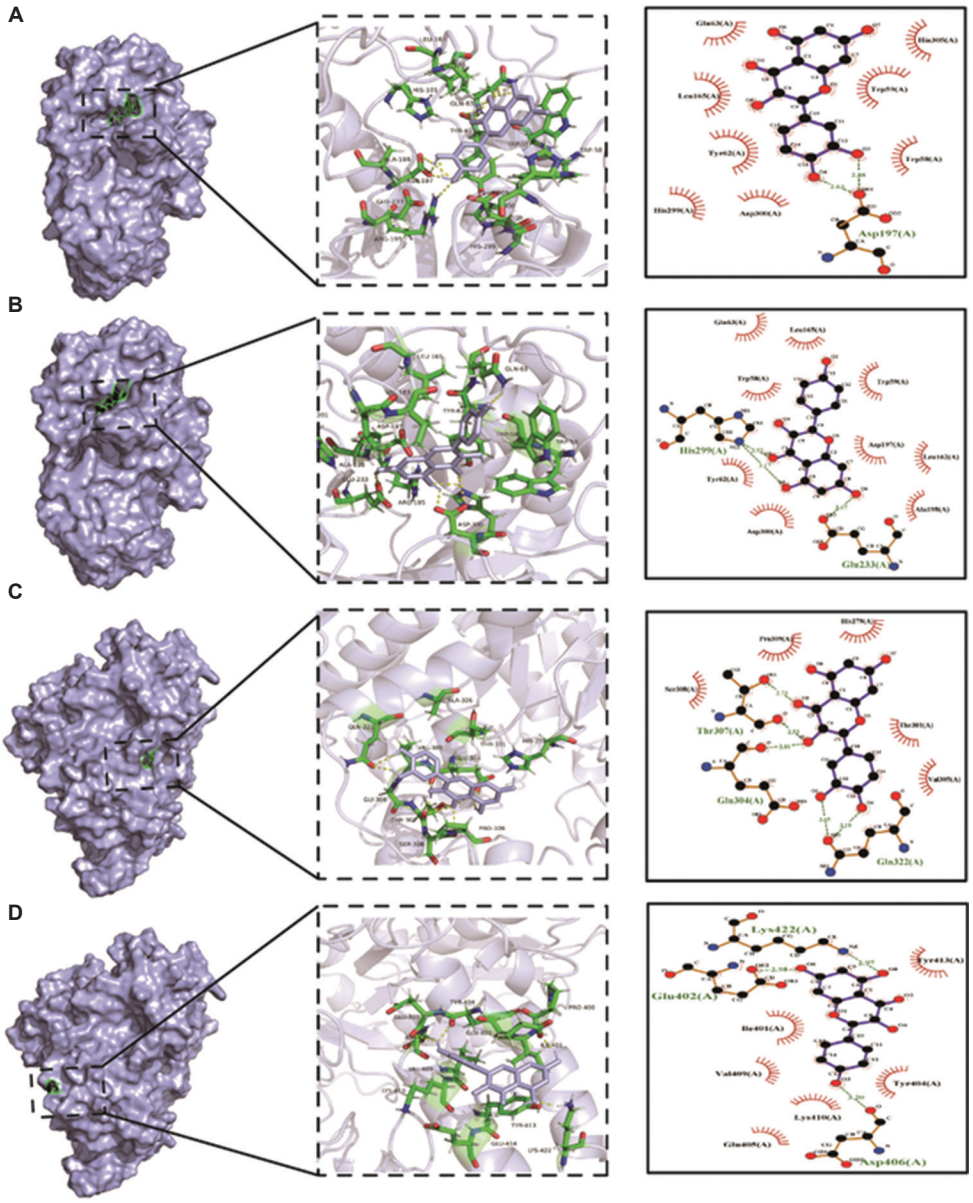

Figure 6. The molecular docking results between quercetin, and kaempferol, and α-amylase/α-glucosidase. The 3D binding diagram of quercetin-α-amylase (A), kaempferol-α-amylase (B), quercetin-α-glucosidase (C), and kaempferol-α-glucosidase (D) (left), and the corresponding 2D interaction diagrams (right).

were −5.7 kcal/mol and −4.63 kcal/mol for α-amylase, respectively, and 5.15 kcal/mol and −5.06 kcal/mol for α-glucosidase (Table 9).[47,48] Thus, from an energetic point of view, quercetin and kaempferol had better binding affinity, which were consistent with the previous correlation analysis and the IC_{50} results for each substance.

As shown in Figure 6, for α-amylase, quercetin formed hydrogen bonds with Asp197 and interacted hydrophobically with Asp300, Gln63, His305, Trp59, Leu165, Tyr62, Trp58, and His299 (Figure 6A). Kaempferol established hydrogen bonding interactions with Glu233 and His299, as well as hydrophobic interactions with residues Asp300, Asp197, Gln63, Trp59, Leu165, Tyr62, Leu16, and Aln198 (Figure 6B). When binding to α-amylase, quercetin and kaempferol impeded the entry of the substrate or occupied the starch binding site, thus further inhibiting α-amylase activity. Asp197, Glu233, and Asp300 were identified as the key active site residues of α-amylase in previous research, and are essential to the catalytic process. The hydrogen bonding interactions of quercetin and kaempferol with these key active site residues

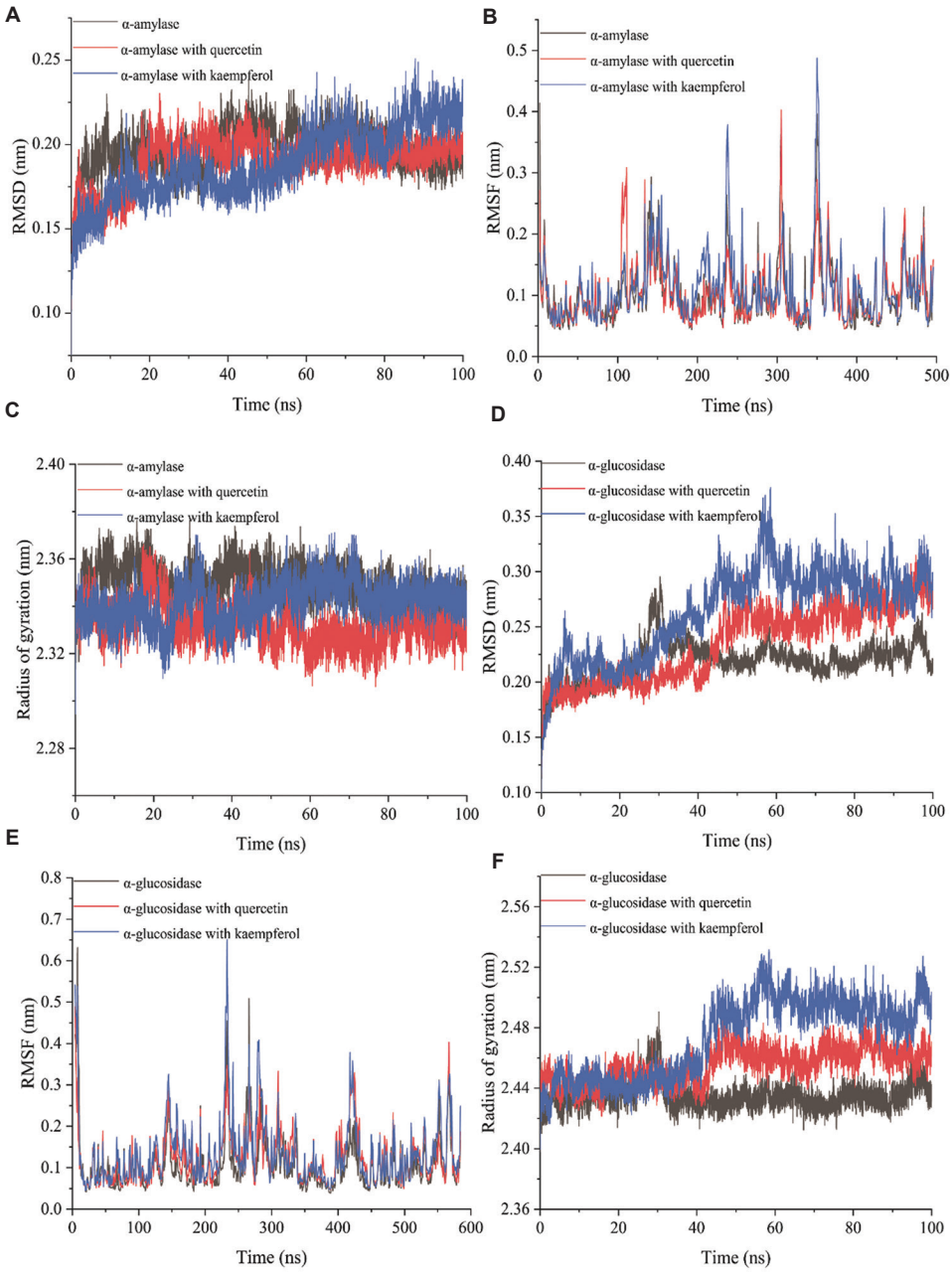

Figure 7. Molecular dynamics simulation of quercetin/kaempferol with α-amylase and α-glucosidase. Molecular dynamics simulations of quercetin and kaempferol with α-amylase (A-C) and α-glucosidase (D-F) for 100 ns.
Abbreviations: RMSD: Root-mean-square deviation; RMSF: Root-mean-square fluctuation.

suggest that they are located within the active cavity of α-amylase. For α-glucosidase, quercetin formed hydrogen bonds with Thr307, Glu304, and Gln322, while forming hydrophobic interactions with His279, Pro309, Ser308, Thr301, and Val305 (Figure 6C). In addition, kaempferol formed hydrogen bonds with Lys422, Glu402 and Asp406, and hydrophobic interactions with Tyr413, Ile401, Val409, Tyr404, Lys410, and Glu405 (Figure 6D). The main active site residues in α-glucosidase, namely Glu277, Asp352, and Glu411, are essential to the catalytic process.[49] However, neither quercetin nor kaempferol interacted directly with these key residues of α-glucosidase, most likely due to their binding around the active site. In conclusion, the flavonoids in FBSJ interact hydrophobically and through hydrogen bonds with both α-amylase and α-glucosidase, significantly influencing their inhibitory activities.[50]

Table 9. Flavonoids in *Sophora japonica* L. molecular docking evaluation table

Number	Compound	α-amylase binding energy (kcal/mol)	α-glucosidase binding energy (kcal/mol)
1	Quercetin	−5.70	−5.15
2	Rutin	−3.71	−3.27
3	Isorhamnetin	−4.54	−4.74
4	Kaempferol-3-O-rutinoside	−3.20	−2.51
5	Kaempferol	−4.63	−5.06
6	Narcissoside	−3.14	−2.19

3.8. MD simulation

The binding stability of quercetin/kaempferol-α-amylase and α-glucosidase complexes was evaluated using root-mean-square deviation (RMSD), root-mean-square fluctuation (RMSF) and radius of gyration (Rg). The results of RMSD were used to evaluate the dynamic stability of the system.[51] In Figure 7A, the free α-amylase stabilized around 10 ns, and the RMSD of the quercetin-α-amylase complex fluctuated in the same region as that of free α-amylase, indicating that quercetin binding only slightly changed the degree of freedom of protein movement, with stability comparable to that of free α-amylase. The RMSD value of the kaempferol-α-amylase complex was significantly higher than that of the quercetin-α-amylase complex, suggesting relatively poorer stability. The flexibility of amino acid is shown in Figure 7B, reflecting the RMSF. During the whole simulation process, the peptide chain from residues 105 – 111 in the quercetin-α-amylase complex fluctuated greatly. The combination of kaempferol and α-amylase caused residues 200 – 213 and 238 to fluctuate greatly. These differences in the protein-ligand complexes reflect the interactions between small molecules and proteins, which changes the protein conformation and may relate to the protein's functional role. Rg is an important parameter to examine the density of the protein structure; the larger the Rg value of the system, the looser the protein structure.[52,53] As shown in Figure 7C, the binding of quercetin reduced the Rg value of α-glucosidase, indicating that quercetin binds to α-glucosidase and forms a more stable system, thus showing significant strong inhibitory activity.

The RMSD value of free α-glucosidase in Figure 7D fluctuated around 0.22 nm, and the RMSD value of the α-glucosidase-kaempferol complex was significantly higher than that of α-glucosidase-quercetin complex. All ligand-α-glucosidase complexes in Figure 7E showed similar fluctuations. Among the Lys233, His 279, and Ser281 residues, the kaempferol-α-glucosidase complex showed higher fluctuations than the quercetin-α-glucosidase complex, indicating that the residue structure was more flexible and unstable. The Rg value of the complex stabilized after 50 ns, as shown in the Rg value in Figure 7F. The binding of both quercetin and kaempferol increased the Rg value of α-glucosidase. The Rg value of the α-glucosidase-kaempferol complex was significantly higher than that of the α-glucosidase-quercetin complex, which made the whole conformation loose and its structure unstable, resulting in a decrease in the catalytic activity of the α-glucosidase active site.

4. Discussion

In this study, we separated and identified six flavonoids from FBSJ and then developed a method to screen their inhibitory effects on α-amylase and α-glucosidase activity *in vitro*. The significance of the inhibition was evaluated through various analytical methods. In addition, we investigated the inhibitory mechanisms through enzyme inhibition kinetics, fluorescence spectrometry, CD, and molecular docking. Our analysis indicated that quercetin and kaempferol were the most effective inhibitors of α-amylase and α-glucosidase, consistent with the IC_{50} and molecular docking results. Both quercetin and kaempferol were found to act as competitive inhibitors against α-amylase and α-glucosidase enzymes. The study revealed that quercetin exhibited a mixed inhibition pattern against α-amylase, while kaempferol demonstrated a mixed inhibition pattern against both α-amylase and α-glucosidase. Fluorescence and CD spectra revealed that flavonoids in FBSJ caused a reduction in fluorescence intensity and structural changes in the enzymes. Molecular docking analysis revealed that quercetin and kaempferol exhibited higher binding energies and tighter interactions with the enzymes. MDs simulations provided further insights into the structure and characteristics of the α-amylase-quercetin/kaempferol complexes and α-glucosidase-quercetin/kaempferol complexes. Notably, the α-amylase/α-glucosidase-quercetin complexes were more stable compared to the α-amylase/α-glucosidase-kaempferol complexes.

5. Conclusion

Based on scoring for significance, the chromatographic analysis CAADA employed in this study proved to be a simple and reliable method. Overall, the findings suggest that quercetin and kaempferol exhibit potential as inhibitors of α-amylase and α-glucosidase in FBSJ.

Acknowledgment

None.

Funding

This research was funded by the National Natural Science Foundation of China (grant number 32161143021).

Conflict of interest

The authors declare that they have no competing interests.

Author contributions

Conceptualization: Yunfeng Ma
Formal analysis: Jiayan Xiong, Jinlin Li, Chaoyang Zhang
Investigation: Yunfeng Ma
Methodology: Jinting Sun, Ranying Zhang, Jiayan Xiong
Writing–original draft: Ranying Zhang
Writing–review & editing: Yunfeng Ma

Ethics approval and consent to participate

Not applicable.

Consent for publication

Not applicable.

Availability of data

Data are available from the corresponding author on reasonable request.

References

1. Zheng Y, Tian J, Yang W, *et al*. Inhibition mechanism of ferulic acid against α-amylase and α-glucosidase. *Food Chem*. 2020;317:126346.

   doi: 10.1016/j.foodchem.2020.126346

2. Hussain T, Tan B, Murtaza G, *et al*. Flavonoids and type 2 diabetes: Evidence of efficacy in clinical and animal studies and delivery strategies to enhance their therapeutic efficacy. *Pharmacol Res*. 2020;152:104629.

   doi: 10.1016/j.phrs.2020.104629

3. Xu X, Wang P, Wang B, *et al*. Glucose absorption regulation and mechanism of the compounds in *Lilium lancifolium* Thunb on Caco-2 cells. *Food Chem Toxicol*. 2021;149:112010.

   doi: 10.1016/j.fct.2021.112010

4. Cui L, Wang J, Wang M, *et al*. Chemical composition and glucose uptake effect on 3T3-L1 adipocytes of *Ligustrum lucidum* Ait. Flowers. *Food Sci Hum Well*. 2020;9(2):124-129.

   doi: 10.1016/j.fshw.2020.02.002

5. Sabiu S, O'Neill FH, Ashafa AOT. Kinetics of α-amylase and α-glucosidase inhibitory potential of *Zea mays* Linnaeus (*Poaceae*), Stigma maydis aqueous extract: An *in vitro* assessment. *J Ethnopharmacol*. 2016;183:1-8.

   doi: 10.1016/j.jep.2016.02.024

6. Han S, Luo Y, Hu Z, D. *et al*. Targeting gut microbiota in type 2 diabetes mellitus: Potential roles of dietary flavonoids. *Food Biosci*. 2022;45:101500.

   doi: 10.1016/j.fbio.2021.101500

7. Bui TT, Nguyen HT. Ethanolic extract of *Sophora japonica* flower buds alleviates cognitive deficits induced by scopolamine in mice. *Oriental Pharm Exp M*. 2017;17(4):337-344.

   doi: 10.1007/s13596-017-0286-6

8. Li J, Gong Y, Li J, *et al*. *In vitro* xanthine oxidase inhibitory properties of Flos Sophorae Immaturus and potential mechanisms. *Food Biosci*. 2022;47:101711.

   doi: 10.1016/j.fbio.2022.101711

9. Liu C, Ma C, Lu J, *et al*. A rapid method and mechanism to identify the active compounds in Malus micromalus Makino fruit with spectrum-effect relationship, components knock-out and molecular docking technology. *Food Chem Toxicol*. 2021;150:112086.

   doi: 10.1016/j.fct.2021.112086

10. Li W, Zhang Y, Shi S, *et al*. Spectrum-effect relationship of antioxidant and tyrosinase activity with *Malus pumila* flowers by UPLC-MS/MS and component knock-out method. *Food Chem Toxicol*. 2019;133:110754.

    doi: 10.1016/j.fct.2019.110754

11. Li F, Fu Y, Yang H, *et al*. The inhibition mechanism of luteolin on peroxidase based on multispectroscopic techniques. *Int J Biol Macromol*. 2021;166:1072-1081.

    doi: 10.1016/j.ijbiomac.2020.10.262

12. Fu M, Shen W, Gao W, *et al*. Essential moieties of myricetins, quercetins and catechins for binding and inhibitory activity against alpha-Glucosidase. *Bioorg Chem*. 2021;115:105235.

    doi: 10.1016/j.bioorg.2021.105235

13. Kazeem MI, Davies TC. Anti-diabetic functional foods as sources of insulin secreting, insulin sensitizing and insulin mimetic agents. *J Funct Foods*. 2016;20:122-138.

    doi: 10.1016/j.jff.2015.10.013

14. Sansenya S, Payaka A, Mansalai P. Biological activity and inhibition potential against α-glucosidase and α-amylase of 2,4-di-tert-butylphenol from bamboo shoot extract by *in vitro* and *in silico* studies. *Process Biochem*. 2023;126:15-22.

15. Xiao Y, Shan X, Wang H, *et al*. Spectrum-effect relationship between HPLC fingerprint and antioxidant of "San-Bai Decoction" extracts. *J Chromatogr B Analyt Technol Biomed Life Sci*. 2022;1208:123380.

    doi: 10.1016/j.jchromb.2022.123380

16. Ma TC, Sun Y, Guo LN, *et al*. Screening potential α-glucosidase inhibitors from *Anemarrhena asphodeloides* using response surface methodology coupled with grey relational analysis. *Chin Herb Med*. 2019;11(1):60-69.

doi: 10.1016/j.chmed.2018.08.010

17. Wu X, Hu M, Hu X, *et al*. Inhibitory mechanism of epicatechin gallate on α-amylase and α-glucosidase and its combinational effect with acarbose or epigallocatechin gallate. *J Mol Liq*. 2019;290:111202.

doi: 10.1016/j.molliq.2019.111202

18. Yang J, Wang X, Zhang C, *et al*. Comparative study of inhibition mechanisms of structurally different flavonoid compounds on alpha-glucosidase and synergistic effect with acarbose. *Food Chem*. 2021;347:129056.

doi: 10.1016/j.foodchem.2021.129056

19. Guo S, Meng J, Wang S, *et al*. Preparation of magnetic microcapsules of α-amylase and α-glucosidase for dual-target affinity screening of active components from *Toona sinensis*. *Process Biochem*. 2023;124:92-99.

doi: 10.1016/j.procbio.2022.11.018

20. Wang R, Fan R, Meng T, *et al*. Exploration of the inhibitory mechanisms of trans-polydatin/resveratrol on α-glucosidase by multi-spectroscopic analysis, *in silico* docking and molecular dynamics simulation. *Spectrochim Acta A Mol Biomol Spectrosc*. 2023;299:122866.

doi: 10.1016/j.saa.2023.122866

21. Wang D, Gu X, Fang K, *et al*. Study on quality control of Zuojin pill by HPLC fingerprint with quantitative analysis of multi-components by single marker method and antioxidant activity analysis. *J Pharm Biomed Anal*. 2023;225:115075.

doi: 10.1016/j.jpba.2022.115075

22. Li C, Cui Y, Lu J, *et al*. Spectrum-effect relationship of immunologic activity of *Ganoderma lucidum* by UPLC-MS/MS and component knock-out method. *Food Sci Hum Wellness*. 2021;10(3):278-288.

doi: 10.1016/j.fshw.2021.02.019

23. Chen Y, Pan G, Xu W, *et al*. Spectrum-effect relationship study between HPLC fingerprints and antioxidant activity of *Sabia parviflora*. *J Chromatogr B Analyt Technol Biomed Life Sci*. 2020;1140:121970.

doi: 10.1016/j.jchromb.2020.121970

24. Zhao Y, Wang M, Huang G. Structure-activity relationship and interaction mechanism of nine structurally similar flavonoids and α-amylase. *J Funct Foods*. 2021;86:104739.

doi: 10.1016/j.jff.2021.104739

25. Wu H, Lv Y, Wei F, Li C, Ge W, Du W. Comparative analysis of anti-osteoporosis efficacy in Radix Dipsaci before and after processing with salt based on spectrum-effect relationship. *J Pharm Biomed*. 2022;221:115078.

doi: 10.1016/j.jpba.2022.115078

26. Yang F, Zou Y, Li C, *et al*. Discovery of potential hypoglycemic metabolites in Cassiae Semen by coupling UHPLC-QTOF-MS/MS combined plant metabolomics and spectrum-effect relationship analyses. *Food Funct*. 2022;13(19):10291-10304.

doi: 10.1039/d2fo00562j

27. Zhang J, Chen T, Li K, *et al*. Screening active ingredients of rosemary based on spectrum-effect relationships between UPLC fingerprint and vasorelaxant activity using three chemometrics. *J Chromatogr B Analyt Technol Biomed Life Sci*. 2019;1134-1135:121854.

doi: 10.1016/j.jchromb.2019.121854

28. Zhang D, Liu X, Yang Z, *et al*. Interactions between phenols and alkylamides of Sichuan Pepper (*Zanthoxylum* genus) in alpha-glucosidase inhibition: A structural mechanism analysis. *J Agric Food Chem*. 2021;69(20):5583-5598.

doi: 10.1021/acs.jafc.1c00741

29. Aleixandre A, Gil JV, Sineiro J, *et al*. Understanding phenolic acids inhibition of α-amylase and α-glucosidase and influence of reaction conditions. *Food Chem*. 2022;372:131231.

doi: 10.1016/j.foodchem.2021.131231

30. Lim J, Ferruzzi MG, Hamaker BR. Structural requirements of flavonoids for the selective inhibition of alpha-amylase versus alpha-glucosidase. *Food Chem*. 2022;370:130981.

doi: 10.1016/j.foodchem.2021.130981

31. Wang S, Li Y, Huang D, *et al*. The inhibitory mechanism of chlorogenic acid and its acylated derivatives on alpha-amylase and α-glucosidase. *Food Chem*. 2022;372:131334.

doi: 10.1016/j.foodchem.2021.131334

32. Ghani U, Nur-e-Alam M, Yousaf M, Ul-Haq Z, Noman OM, Al-Rehaily AJ. Natural flavonoid α-glucosidase inhibitors from Retama raetam: Enzyme inhibition and molecular docking reveal important interactions with the enzyme active site. *Bioorg Chem*. 2019;87:736-742.

doi: 10.1016/j.bioorg.2019.03.079

33. Wang Y, Zhang G, Pan J, *et al*. Novel insights into the inhibitory mechanism of kaempferol on xanthine oxidase. *J Agric Food Chem*. 2015;63(2):526-534.

doi: 10.1021/jf505584m

34. Hua F, Zhou P, Wu HY, *et al*. Inhibition of α-glucosidase and α-amylase by flavonoid glycosides from Lu'an GuaPian tea: Molecular docking and interaction mechanism. *Food Funct*. 2018;9(8):4173-4183.

doi: 10.1039/c8fo00562a

35. Wu Y, Han Z, Wen M, *et al*. Screening of α-glucosidase inhibitors in large-leaf yellow tea by offline bioassay coupled with liquid chromatography tandem mass spectrometry. *Food Sci Hum Well*. 2022;11(3):627-634.

doi: 10.1016/j.fshw.2021.12.019

36. Sun L, Chen W, Meng Y, *et al*. Interactions between polyphenols in thinned young apples and porcine pancreatic α-amylase: Inhibition, detailed kinetics and fluorescence quenching. *Food Chem*. 2016;208:51-60.

doi: 10.1016/j.foodchem.2016.03.093

37. Wang S, Xie X, Zhang L, *et al*. Inhibition mechanism of α-glucosidase inhibitors screened from *Artemisia selengensis* Turcz root. *Ind Crop Prod*. 2020;143:111941.

doi: 10.1016/j.indcrop.2019.111941

38. Wang L, Wang L, Wang T, *et al*. Comparison of quercetin and rutin inhibitory influence on Tartary buckwheat starch digestion *in vitro* and their differences in binding sites with the digestive enzyme. *Food Chem*. 2022;367:130762.

doi: 10.1016/j.foodchem.2021.130762

39. Yan J, Zhang G, Pan J, Wang Y. α-Glucosidase inhibition by luteolin: Kinetics, interaction and molecular docking. *Int J Biol Macromol*. 2014;64:213-223.

doi: 10.1016/j.ijbiomac.2013.12.007

40. Wang Q, Li R, Li N, *et al*. The antioxidant activities, inhibitory effects, kinetics, and mechanisms of artocarpin and alpha-mangostin on alpha-glucosidase and alpha-amylase. *Int J Biol Macromol*. 2022;213:880-889.

doi: 10.1016/j.ijbiomac.2022.06.017

41. Yang Y, Zhang P, Huang Z, *et al*. Phenolics from *Sterculia nobilis* Smith pericarp by-products delay carbohydrate digestion by uncompetitively inhibiting α-glucosidase and α-amylase. *LWT*. 2023;173:114339.

doi: 10.1016/j.lwt.2022.114339

42. Yu Q, Fan L, Duan Z. Five individual polyphenols as tyrosinase inhibitors: Inhibitory activity, synergistic effect, action mechanism, and molecular docking. *Food Chem*. 2019;297:124910.

doi: 10.1016/j.foodchem.2019.05.184

43. Song X, Ni M, Zhang Y, Zhang G, Pan J, Gong D. Comparing the inhibitory abilities of epigallocatechin-3-gallate and gallocatechin gallate against tyrosinase and their combined effects with kojic acid. *Food Chem*. 2021;349:129172.

doi: 10.1016/j.foodchem.2021.129172

44. Ding H, Wu X, Pan J, *et al*. New insights into the inhibition mechanism of betulinic acid on α-glucosidase. *J Agric Food Chem*. 2018;66(27):7065-7075.

doi: 10.1021/acs.jafc.8b02992

45. Peng X, Zhang G, Liao Y, *et al*. Inhibitory kinetics and mechanism of kaempferol on alpha-glucosidase. *Food Chem*. 2016;190:207-215.

doi: 10.1016/j.foodchem.2015.05.088

46. Han L, Song J, Yan C, *et al*. Inhibitory activity and mechanism of calycosin and calycosin-7-O-β-D-glucoside on α-glucosidase: Spectroscopic and molecular docking analyses. *Process Biochem*. 2022;118:227-235.

doi: 10.1016/j.procbio.2022.04.035

47. Shen H, Wang J, Ao J, *et al*. Structure-activity relationships and the underlying mechanism of alpha-amylase inhibition by hyperoside and quercetin: Multi-spectroscopy and molecular docking analyses. *Spectrochim Acta A Mol Spectrosc*. 2023;285:121797.

doi: 10.1016/j.saa.2022.121797

48. Li M, Bao X, Zhang X, *et al*. Exploring the phytochemicals and inhibitory effects against α-glucosidase and dipeptidyl peptidase-IV in Chinese pickled chili pepper: Insights into mechanisms by molecular docking analysis. *LWT*. 2022;162:113467.

doi: 10.1016/j.lwt.2022.113467

49. Han L, Fang C, Zhu R, *et al*. Inhibitory effect of phloretin on alpha-glucosidase: Kinetics, interaction mechanism and molecular docking. *Int J Biol Macromol*. 2017;95:520-527.

doi: 10.1016/j.ijbiomac.2016.11.089

50. Zhang J, Ding W, Tang Z, *et al*. Identification of the effective alpha-amylase inhibitors from *Dalbergia odorifera*: Virtual screening, spectroscopy, molecular docking, and molecular dynamic simulation. *Spectrochim Acta A Mol Biomol Spectrosc*. 2022;280:121448.

doi: 10.1016/j.saa.2022.121448

51. Phong NV, Yang SY, Min BS, *et al*. Insights into the inhibitory activity and mechanism of action of flavonoids from the stems and branches of *Acer mono* Maxim. Against α-glucosidase via kinetic analysis, molecular docking, and molecular dynamics simulations. *J Mol Struct*. 2023;1282:135188.

doi: 10.1016/j.molstruc.2023.135188

52. Yadav R, Hasan S, Mahato S, *et al*. Molecular docking, DFT analysis, and dynamics simulation of natural bioactive compounds targeting ACE2 and TMPRSS2 dual binding sites of spike protein of SARS CoV-2. *J Mol Liq*. 2021;342:116942.

doi: 10.1016/j.molliq.2021.116942

53. Sharifpour S, Fakhraee S, Behjatmanesh-Ardakani R. Insights into the mechanism of inhibition of phospholipase A2 by resveratrol: An extensive molecular dynamics simulation and binding free energy calculation. *J Mol Graph Model*. 2020;100:107649.

doi: 10.1016/j.jmgm.2020.107649